Journal of Physics: Conference Series **3177** (2026) 012066 doi:10.1088/1742-6596/3177/1/012066

Gravitational waves from supermassive black holes at pulsar timing arrays

Ville Vaskonen[1,2]

[1]Dipartimento di Fisica e Astronomia, Università degli Studi di Padova, and Istituto Nazionale di Fisica Nucleare, Sezione di Padova, Via Marzolo 8, 35131 Padova, Italy

[2]Keemilise ja Bioloogilise Füüsika Instituut, Rävala pst. 10, 10143 Tallinn, Estonia

E-mail: ville.vaskonen@pd.infn.it

Abstract. Inspiralling supermassive black hole binaries are a natural explanation for the gravitational wave background detected in pulsar timing array data. We have developed a fast and accurate method for computing the gravitational wave background from supermassive black hole binaries, and applied it to analyze the pulsar timing array data, finding strong evidence for environmental effects or binary eccentricities. This proceedings article, based on a talk given at the GR24–Amaldi16 conference, summarizes these results.

1 Introduction

The pulsar timing arrays (PTAs) have found strong evidence for a gravitational wave background (GWB) at the nHz range [1, 2, 3, 4]. A natural astrophysical interpretation of such background is GW emission by supermassive black hole (SMBH) binaries. An SMBH pair is put together by a galaxy merger. The separation of the pair shrinks through interactions with its environment such as dynamical friction and scattering off stars (see e.g. [5]). The pair eventually becomes a bound binary whose evolution at sub-parsec separations is determined by GW emission. The merger rate of SMBH binaries can be estimated from the merger rate R_h of DM halos, computed e.g. from the EPS formalism, as (see e.g. [6, 7])

$$\frac{\mathrm{d}R_{\rm BH}}{\mathrm{d}m_1\mathrm{d}m_2} = p_{\rm BH}\int \mathrm{d}M_1\mathrm{d}M_2\,\frac{\mathrm{d}R_h}{\mathrm{d}M_1\mathrm{d}M_2}\prod_{j=1,2}\frac{\mathrm{d}P(m_j|M_j)}{\mathrm{d}m_j}\,. \tag{1}$$

The prefactor $0 < p_{\rm BH} \leq 1$ quantifies the probability that a halo merger forms an SMBH binary, and $\mathrm{d}P(m_j|M_j)/\mathrm{d}m_j$ denotes the distribution of SMBH masses m_j in dark matter halos of mass M_j. The latter can be estimated in two steps: first relating the dark matter halo masses to galaxy stellar masses, e.g. through observations of galaxy luminosity functions [8, 9], and then relating the stellar masses to halo masses. As the SMBHs contributing to the GWB at nHz frequencies are dominated by the heaviest SMBHs [6], $m_j > 10^8 M_\odot$, at $z \lesssim 1$, the stellar mass-BH mass relation can be estimated from the observations of local inactive galaxies [10, 11].

2 Distribution of SMBH GWB realizations

The mean GWB from SMBH binaries is given simply by

$$\langle \Omega_{\rm tot} \rangle = \int {\rm d}\lambda \frac{{\rm d}t_c}{{\rm d}\ln f} \Omega^{(1)} \,, \tag{2}$$

where ${\rm d}\lambda \propto {\rm d}R_{\rm BH}$ denotes the merger rate of SMBH binaries in a comoving volume, $\Omega^{(1)}_{\rm GW} \propto (\mathcal{M}f)^{10/3} D_L^{-2}$ the contribution to the GWB from a single binary with a chirp mass $\mathcal{M}$ at luminosity distance D_L and ${\rm d}t_c/{\rm d}\ln f \propto (1+z)\mathcal{M}^{-5/3} f^{-8/3}$ describes how quickly the binary frequency evolves. For GW-driven binaries, the mean is a power-law $\langle \Omega_{\rm tot} \rangle \propto f^{2/3}$. A realization of the SMBH GWB can be obtained by generating a population of SMBH binaries from the SMBH merger rate and summing the contributions from each binary:

$$\Omega_{\rm tot}(f_i) = \sum_{j=1}^{N(f_i)} \Omega^{(1)}_j \,. \tag{3}$$

Two realizations of the GWB are shown in the left panel of Fig. 1 by the blue solid and dashed curves. Compared to the mean shown by the black curve, these realizations typically lie at lower amplitudes, but at some frequencies, they can include large upwards fluctuations that reach above the mean. These upwards fluctuations are caused by nearby binaries.

The violins in the left panel of Fig. 1 show the distributions of possible SMBH GWB realizations at different frequencies. The distribution can be obtained by generating a large number of realizations of the SMBH binary population. Accurate estimation of the distributions in this way is, however, computationally slow. A fast and accurate computation of the SMBH GWB distributions was derived in Refs. [6, 7] and extended to eccentric binaries and to studies of anisotropies in [12, 13]. First, instead of generating the binary parameters, including the chirp masses and luminosity distance, from the merger rate, we can directly generate single binary contributions Ω to the SMBH GWB from the distribution

$$P^{(1)}(\Omega) \propto \int {\rm d}\lambda \frac{{\rm d}t}{{\rm d}\ln f_r} \delta(\Omega - \Omega^{(1)}) \,. \tag{4}$$

Furthermore, we can divide the contributions into weak and strong ones by setting a threshold value on $\Omega^{(1)}$ e.g. so that the number of strong contributions N_S is fixed. Then, only the N_S strong contributions with $\Omega^{(1)} > \Omega_{\rm thr}$ need to be generated and the distribution of their sum $\Omega_{\rm strong} = \sum_{j=1}^{N_S} \Omega^{(1)}_j$ can be computed by generating many realizations of the strong contributions. The distribution of the total contribution from weak sources is a narrow Gaussian whose mean is obtained as in Eq. (2) with a threshold $\Omega^{(1)} < \Omega_{\rm thr}$. The distribution of $\Omega_{\rm tot} = \Omega_{\rm weak} + \Omega_{\rm strong}$ can then be approximated by shifting the distribution of the strong sources by the mean of the weak sources.

The gray dashed curve in the right panel of Fig. 1 shows $\bar{N} P^{(1)}(\Omega)$. The distribution of single binary contributions $P^{(1)}$ asymptotes to a power-law $P^{(1)} \propto \Omega^{-5/2}$ at high values of Ω. This power-law tail

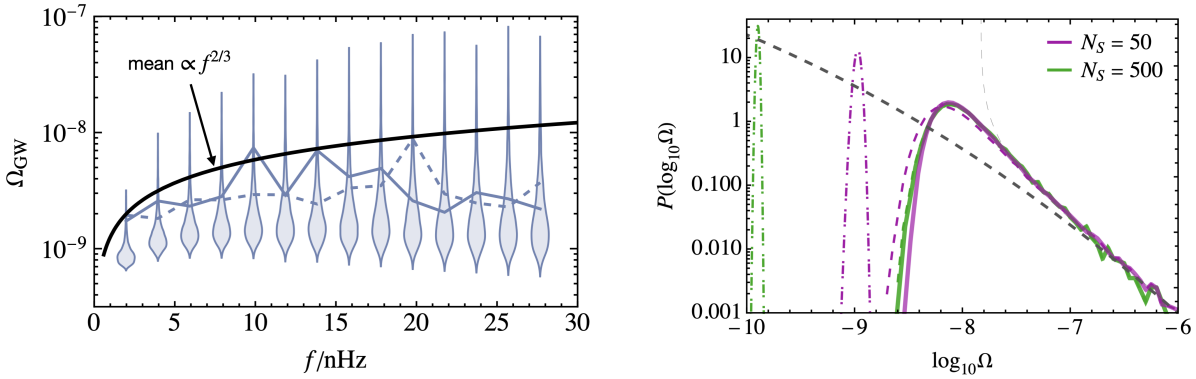

Figure 1: *Left panel:* The blue solid and dashed curves show two realizations of the SMBH GWB for GW-driven circular binaries, the violins show the distribution of possible realizations at different frequency bins, and the black curve shows the mean of these distributions. *Right panel (from [7]):* The green and purple solid curves show the distribution of the SMBH GWB realizations at a frequency bin for two choices of the cutoff between weak and strong sources, whose contributions are indicated by the dot-dashed and dashed curves. The dashed gray curve shows the distribution of single binary contributions.

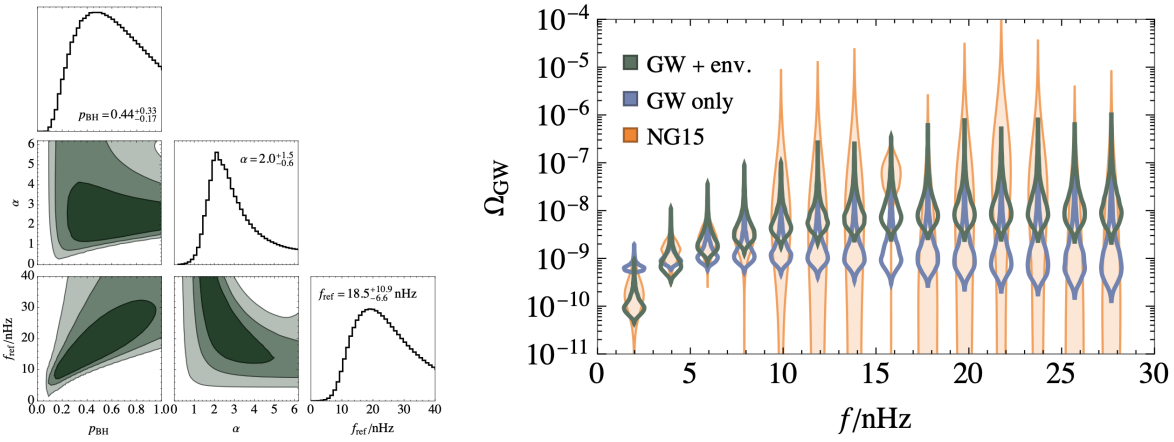

Figure 2: The posteriors of the PTA fit in the model including environmental effects to circular SMBH binaries and the best fits in the GW-driven model and in the model with environmental effects, compared to the PTA data (from [7]).

arises from the possibility of having nearby sources [6]. Notice that this is not affected by how the SMBH merger rate is estimated, as the merger rate in general does not change rapidly with redshift in the local universe. The distribution of $\Omega_{\rm tot}$ also has the same power-law tail, and, consequently, only the first moment of $P(\Omega_{\rm tot})$ is finite. The distribution $P(\Omega_{\rm tot})$ is shown in the right panel of Fig. 1 by the solid green and purple curves for two choices of the threshold $\Omega_{\rm thr}$ that correspond to $N_S = 50$ and 500. We see that the higher threshold that corresponds to $N_S = 50$ already gives a good estimate of the distribution.

3 PTA fit of the SMBH GWB

With the accurate and fast method of computing the distributions $P(\Omega_{\rm tot}|f_j)$ at different GW frequencies f_j predicted by the model, we can perform a likelihood analysis of the model parameters against the observed data. The likelihood is given by $\mathcal{L}(\vec{\theta}) = \prod_{j=1}^{N_f} \int {\rm d}\Omega_{\rm tot} P_{\rm data}(\Omega_{\rm tot}|f_j) P(\Omega_{\rm tot}|f_j, \vec{\theta})$, where $P_{\rm data}(\Omega_{\rm tot}|f_j)$ are the distributions inferred from the observations of the timing residuals. The best fit assuming GW-driven binaries is shown in the right panel of Fig. 2 with the blue violins. Compared to the data shown by the yellow violins, we see that this model seems to predict a too flat spectrum. A better fit is obtained if the spectrum would be suppressed at the lowest frequency bins. Such suppression can be naturally realized including environmental effects that drive the evolution of the binary at those frequencies or binary eccentricities due to which the binaries evolve faster at the lowest frequencies and emit GWs at frequencies integer multiples of their orbital frequency (see [14] for a review). The best fit in the model including environmental effects is significantly better than in the GW-only driven model, as seen in the right panel of Fig. 2. The left panel of Fig. 2 shows the posterior of the model including environmental effects parametrized with two parameters: the reference frequency $f_{\rm ref}$ below which the environmental effects determine the binary evolution, and the power α that determines how the effective timescale of the environmental effects scales with frequency, $t_{\rm env} \propto f^\alpha$ at $f < f_{\rm ref}$. We see that the environmental effects are needed up to quite high frequencies $f_{\rm ref} \gtrsim 10\,{\rm nHz}$ [7], and the environmental effects model is favoured over the GW-only model, corresponding to the limit $f_{\rm ref} \to 0$, by more than 3σ. A similar fit can be obtained including eccentricities in the GW-only model, and a good fit is obtained with relatively large eccentricities of $\langle e \rangle_{2\,{\rm nHz}} \gtrsim 0.6$ [12].

4 Summary

We have developed a fast and accurate method for the computation of the distribution of GWB realizations from SMBH binaries. We have shown that this distribution has a power-law tail $P \propto \Omega^{-5/2}$ at large Ω. Consequently, only the first moment of this distribution is finite. We have used this method to analyze the PTA data, adopting a model where the SMBH merger rate is obtained from the halo merger rate estimated in the EPS formalism. We have included environmental effects and eccentricities that affect the binary evolution and GW emission. We have shown that the data prefers models with strong environmental effects or highly eccentric binaries.

References

[1] Agazie G *et al.* (NANOGrav) 2023 ApJ **951** L8 (*Preprint* 2306.16213)

[2] Antoniadis J *et al.* (EPTA, InPTA) 2024 A&A **685** A94 (*Preprint* 2306.16227)

[3] Reardon D J *et al.* 2023 ApJ **951** L6 (*Preprint* 2306.16215)

[4] Xu H *et al.* 2023 *Res. Astron. Astrophys.* **23** 075024 (*Preprint* 2306.16216)

[5] Kelley L Z, Blecha L and Hernquist L 2017 *Mon. Not. Roy. Astron. Soc.* **464** 3131–3157 (*Preprint* 1606.01900)

[6] Ellis J, Fairbairn M, Hütsi G, Raidal M, Urrutia J, Vaskonen V and Veermäe H 2023 A&A **676** A38 (*Preprint* 2301.13854)

[7] Ellis J, Fairbairn M, Hütsi G, Raidal J, Urrutia J, Vaskonen V and Veermäe H 2024 Phys. Rev. D **109** L021302 (*Preprint* 2306.17021)

[8] Girelli G, Pozzetti L, Bolzonella M, Giocoli C, Marulli F and Baldi M 2020 A&A **634** A135 (*Preprint* 2001.02230)

[9] Ellis J, Fairbairn M, Urrutia J and Vaskonen V 2024 (*Preprint* 2410.24224)

[10] Kormendy J and Ho L C 2013 ARA&A **51** 511–653 (*Preprint* 1304.7762)

[11] Reines A E and Volonteri M 2015 ApJ **813** 82 (*Preprint* 1508.06274)

[12] Raidal J, Urrutia J, Vaskonen V and Veermäe H 2024 A&A **691** A212 (*Preprint* 2406.05125)

[13] Raidal J, Urrutia J, Vaskonen V and Veermäe H 2024 (*Preprint* 2411.19692)

[14] Sesana A 2013 *Class. Quant. Grav.* **30** 224014 (*Preprint* 1307.2600)